Romanian Reports in Physics, Vol. 63, No. 3, P. 817–822, 2011

SPECTROSCOPIC INVESTIGATION OF Sm^{3+} IN YAG CERAMIC

A. LUPEI[1], V. LUPEI[1], C. GHEORGHE[1], A. IKESUE[2]

[1]National Institute of Lasers, Plasma and Radiation Physics, Magurele- Bucharest, R -077125, Romania, lupei_aurelia@yahoo.com
[2]World-Lab. Co. Ltd., Atsuta-ku, Nagoya 456-8587, Japan

Received February 15, 2011

Abstract. An analysis of the high resolution optical spectra (at 10 or 300 K) of Sm^{3+} in YAG transparent ceramics is presented. The peculiarities of the spectra in ceramics are outlined. Accurate data for the application of Sm^{3+}: YAG ceramic to suppress parasitic oscillations in high power Nd: YAG ceramic composite lasers are obtained.

Key words: Sm^{3+}, YAG ceramic, optical spectroscopy.

1. INTRODUCTION

In the search of new laser materials or phosphors, the spectroscopic characteristics of many rare earths ions in different hosts have been investigated. Though Sm^{3+} ($4f^5$) ion presents strong emissions in visible, with long lifetimes (msec) at low concentrations, the interest for this ion was insignificant for many years. The main reason is that pumping is limited by low intensity absorption spectra, unfavorable for efficient excitation with the existing sources and the increase of absorption by large dopings leads to luminescence quenching by cross-relaxation on intermediate levels. However, in the last few years, the interest in using Sm^{3+} efficient emission in various materials, especially for fosphors in red – orange, but also for laser emission has increased in connection with the development of lasers diodes in the 405 nm range, used already in many applications (lighting, optical storage, etc.). Several spectral characteristics of Sm^{3+} in YAG ($Y_3Al_5O_{12}$) single crystals have been measured, such as the energy level scheme [1, 2] (with divergences in many spectral ranges, especially in visible-u.v.); radiative characteristics, lifetimes, etc. [2]. Sm^{3+}: YAG emission has been also investigated for static ultrahigh pressure sensors at high temperatures [3, 4].

The YAG ($Y_3Al_5O_{12}$) transparent ceramics doped with different trivalent rare earth RE^{3+} ions (Nd^{3+}, Yb^{3+}, Er^{3+}, Tm^{3+}, etc) revealed important characteristics that open new possibilities in designing the laser medium with respect to dopant

concentration, distribution, size and geometry [5]. Up to now, there is no systematic study of the spectral features of Sm^{3+} ion in YAG transparent ceramics. Fabrication of transparent Sm: YAG ceramics with concentrations much larger (5 at. %) than for single crystals (2-3 at. %) was reported and a low resolution spectrum at 300 K [6] revealed that the main 1064.15 nm luminescence of Nd^{3+} in YAG can be absorbed in a wing of an absorption line peaking at ~1065.5 nm and has very weak absorption in the 800-900 nm range (diode pumping range of Nd: YAG). Based on this, Sm: YAG has been proposed for suppresion of parasitic oscillations caused by the amplified spontaneous emission (ASE) of the residual luminescence of Nd^{3+}, facilitated by reflection on the laser rod's edges in high storage or large aperture end- or edge-diode laser pumped Nd: YAG lasers [6]. Since there are no large differences between the refraction indices of YAG doped with various RE^{3+} ions, composite Sm^{3+}:YAG/Nd^{3+}:YAG materials could be used as suppressors for Nd^{3+} ASE. The ceramic techniques enable fabrication of monolithic composite materials, with the core-doped ceramic Nd: YAG surrounded by Sm: YAG cladding. Such monolithic composite rods [7, 8] demonstrated the suppression of the parasitic oscillations in diode laser end-pumped Q-switched Nd: YAG lasers, and composite slabs [9], used in diode laser edge-pumped large aperture heat-capacity high power burst regime laser experiments. Owing to the dense structure of energy manifolds in Sm^{3+} it could be expected that all Nd^{3+} luminescence absorbed by Sm^{3+} would be transformed into heat, that could induce distortion of the front wave of the Nd^{3+} laser. Thus, in order to grant high absorption efficiency of the Nd^{3+} luminescence and to control the thermal field induced by the non-radiative de-excitation, a detailed knowledge of the spectroscopic properties of Sm^{3+}: YAG ceramics would be necessary.

This note reports the results of a preliminary investigation of the spectral features of Sm^{3+} in YAG ceramics by using high resolution measurements at 10 and 300 K and evaluation of several spectral characteristics of relevance for suppression of ASE in Nd:YAG lasers, in relation with the previous reported data on single crystals [1, 2] or ceramics [6].

2. EXPERIMENTAL DETAILS

The (1at. %) Sm: YAG ceramic samples used in this investigation were prepared by solid state synthesis [10] The optical spectroscopic measurements include: high resolution absorption and emission at 10 and 300 K. The spectral set - up contains: tungsten halogen or xenon lamps as excitation sources, 1-meter Jarell-Ash monochromator, S_{20} and S_1 phomultipliers or diodes as detectors for i.r. or visible, a Lock – in SRS amplifier connected to a computer and a closed cycle He refrigerator ARS-2HW.

3. RESULTS AND DISCUSSION

The Sm^{3+} ions in YAG ($Y_3Al_5O_{12}$) replace Y^{3+} ions in dodecahedral sites. The energy levels scheme of Sm^{3+} in YAG is complex, with many close manifolds, from near IR to u.v.; part of this scheme is shown in Fig. 1. The metastable level $^4G_{5/2}$ presents a gap of ~ 6830 cm^{-1} to the next lower level $^6F_{11/2}$. Above the $^4G_{5/2}$ (17 601, 17 870, 17 884 cm^{-1}) manifold there is a dense packing of energy manifolds whose Stark levels intermix, making the assignment of the spectral lines difficult.

The Sm: YAG ceramic absorption spectra between 6 000–26 000 cm^{-1} are dominated by the lines corresponding to Sm^{3+} in D_2 sites, the most intense lines being in near IR and correspond to $^6H_{5/2} \rightarrow {}^6F_{5/2,}$ $^6H_{5/2} \rightarrow {}^6F_{7/2}$ and $^6H_{5/2} \rightarrow {}^6F_{9/2}$ transitions. Figure 2 presents 10 and 300 K absorptions connected to $^6H_{5/2} \rightarrow {}^6F_{7/2}$ and $^6H_{5/2} \rightarrow {}^6F_{9/2}$ transitions. The spectra evidence strong temperature dependences of the peak intensities and linewidths, but quite insignificant (within ~ 1 cm^{-1}) red shifts of the lines between 10 to 300 K. The peak absorption cross sections for most intense lines at 300 K in i.r. are: ~ 2.3×10^{-20} cm^2 at 1 225 nm, ~ 1.6×10^{-20} cm^2 at ~ 1068 nm, ~ 0.56×10^{-20} cm^2 at 1065.5 nm. The visible – u.v. absorption spectra above $^6H_{5/2} \rightarrow {}^5G_{5/2}$ lines are complex, with rather small absorption intensities that makes the previous assignments of levels quite different [1, 2]. There is, however, a group of more intense absorption lines around 405 nm, in the range of GaN laser diode emission. The multitude of intermediate levels favors fast population of the metastable level $^5G_{5/2}$ by non-radiative processes from the upper levels.

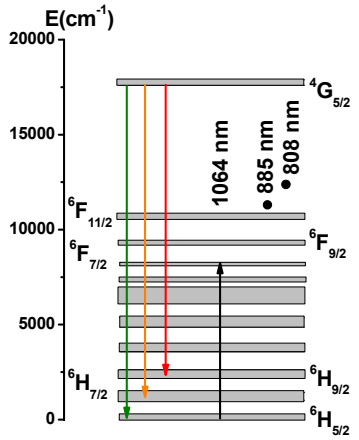

Fig. 1 – Part of the energy level scheme of Sm^{3+} in YAG ceramic.

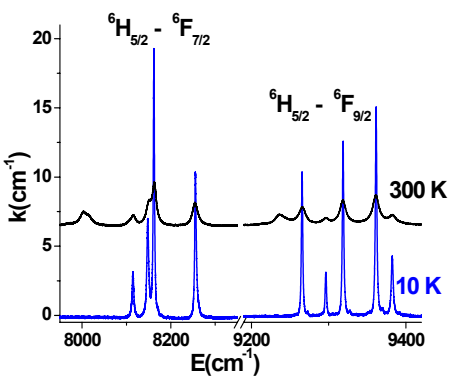

Fig. 2 – $^6H_{5/2} \rightarrow {}^6F_{7/2}$ and $^6H_{5/2} \rightarrow {}^6F_{9/2}$ absorption at 10 and 300 K of Sm^{3+} (1at. %): YAG ceramic.

The emission spectra under filtered lamp excitation correspond to transitions from the metastable $^4G_{5/2}$ level (Fig. 1), the most intense lines being $^4G_{5/2} \rightarrow {}^6H_{5/2}$ (~ 570nm), $^4G_{5/2} \rightarrow {}^6H_{7/2}$ (~ 617 nm, the strongest emission) and $^4G_{5/2} \rightarrow {}^6H_{9/2}$ (~ 650 nm) transitions. The $^4G_{5/2} \rightarrow {}^6H_{7/2}$ emission spectrum of Sm: YAG can be used for high pressure calibration [3, 4], even at high temperatures, since its pressure shift is as large as the ruby R_1 line [3, 4] but shows much smaller temperature variations in position. The small temperature shifts of the lines in Sm^{3+}:YAG, not analyzed previously, could be linked with the small electron-phonon coupling for the RE^{3+} ions in the middle of the lanthanide series [11, 12].

Based on the absorption and emission spectra an improved energy level scheme for Sm^{3+} in YAG ceramic was obtained; the Stark components for several manifolds (interesting for visible emission or for absorption in the 1 and 0.9 micron range) are given in Table 1. The Stark levels positions are similar (within several cm^{-1}) to those reported for single crystals in [1, 2], with larger discrepancies in $^6H_{11/2}$, $^6F_{7/2}$ manifolds.

Besides the lines assigned to Sm^{3+} in D_2 sites, the only additional features observed in ceramics are small satellites accompanying the main intense lines (as observed in 10 K spectra presented in Fig. 2). They were detected on both sides of the D_2 lines, with shifts in the range of ~ ±(6 – 10) cm^{-1}, depending on transition, and peak relative intensities to the main lines smaller than ~0.025. Such satellites have been remarked in Sm^{3+}:YAG single crystals too [1], without clear assignment. High-resolution spectroscopic investigation of the RE^{3+} ions in melt-grown YAG crystals [13, 14] revealed two types of satellite structures, caused either by crystal field perturbations produced by the excess Y^{3+} ions, which enter in octahedral sites occupied normally by Al^{3+} ions (four satellites P_i [15]) or by crystal field perturbations inside statistical ensembles of doping ions in near lattice sites, mostly nearest-neighbor (n.n.) and next-nearest-neighbor (n.n.n.) pairs (satellites M_1 and M_2) [14, 16]. At low doping concentrations the absolute intensities of satellites P_i as well as that of the unperturbed main line N scale linearly with the doping concentration, whereas that of the pair satellites M_i increase quadratically. It was subsequently shown [17, 18] that the concentration of non-stoichiometric defects in the Nd-doped YAG ceramics is much lower than in single crystals and this was linked to the lower (by about 300^0C) fabrication temperature.

Table 1

Several energy levels in the i.r. range of Sm^{3+}: YAG ceramic

Manifold	Stark Levels (cm^{-1})
$^6H_{5/2}$	0, 141, 252
$^6H_{7/2}$	1020, 1239, 1369, 1416
$^6H_{9/2}$	2256, 2403, 2468, 2570, 2621
$^6H_{11/2}$	3559, 3645, 3759, 3827, 3874, 3 943
$^6F_{7/2}$	8155, 8148, 8162, 8256
$^6F_{9/2}$	9266, 9297, 9319, 9362, 9383
$^6F_{11/2}$	10601, 10622, 10675, 10707, 10742, 10767

Sm^{3+}:YAG presents at 300 K absorption in the 1 050 nm–1 100 nm domain, on $^6H_{5/2} \rightarrow {}^6F_{9/2}$ transitions (Fig. 3), but no absorption was observed at 808 or 885 nm, the laser diodes emission wavelengths used for Nd: YAG pumping (Fig. 1). The small absorption at 808 nm reported previously for Sm (5at. %): YAG ceramics [6] should have other origin.

The overlap of Nd^{3+}: YAG $^4F_{3/2} \rightarrow {}^4I_{11/2}$ emission with Sm^{3+} $^6H_{5/2} \rightarrow {}^6F_{9/2}$ absorption that determines the efficiency of Sm: YAG as ASE suppressor for Nd: YAG at 300 K is presented in Fig. 3, showing that many Nd^{3+} emission lines could be absorbed. At 300 K the main Nd^{3+} emission line (1 064.15 nm) is absorbed only on a tail of the Sm^{3+} 1 065.5 nm line, and the estimated absorption coefficient for (1at.%) Sm^{3+} is ~ 0.15 cm^{-1}.

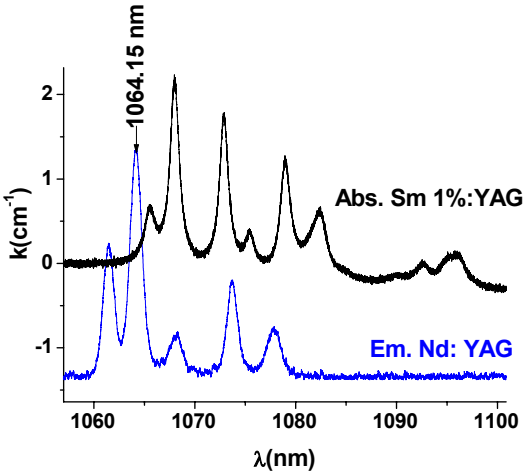

Fig. 3 – Overlap of the Nd: YAG $^4F_{3/2} \rightarrow {}^4I_{11/2}$ emission with $^6H_{5/2} \rightarrow {}^6F_{9/2}$ Sm(1at. %): YAG absorption at 300 K.

Low temperature high-resolution measurements (Fig. 2) evidence a spectral satellite shifted by ~ 1 nm on the low wavelength side of Sm: YAG $^6H_{5/2}(1) \rightarrow {}^6F_{9/2}(5)$ absorption line, i.e. closer to the 1064.15 nm Nd^{3+} emission. The peak relative intensity of this satellite is ~0.2 to that of the main line, but its linewidth seems larger. The origin of this satellite is not clear: the existence of a unique satellite does not favor its assignment as P_i satellite and its intensity is much over the values for other RE^{3+} ions in YAG ceramics, where these satellites are barely observable. On other hand, this satellite resembles the M_1 satellite of other RE^{3+} in YAG, although its spectral shift from the line N is unusually large [16]. At 300K such satellite contributes, together with the concentration broadening and with the electron-phonon broadening to the tail of the $^6H_{5/2}(1) \rightarrow {}^6F_{9/2}(5)$ absorption line. By extrapolating the absorption coefficient at 1064.15 nm measured in this work to the

high Sm^{3+} concentration (5 at.%) assuming that this satellite is of *P* type would give an absorption coefficient of ~0.75 cm^{-1}, much smaller than the value of 3.6 cm^{-1} reported previously for Sm in YAG ceramic [6]. If this Sm^{3+} satellite (at 1 064.15 nm) is due to a n.n. pair, its extrapolated absorption coefficient at 5 at.% Sm could be ~3.75 cm^{-1}. Nevertheless, a definite answer to the differences from data of Ref. [6] (experimental resolution or sample concentration effects) would require measurements on samples of higher Sm^{3+} concentration.

In conclusion, the preliminary results of the high resolution investigation of Sm: YAG ceramic indicate that although the 1 064.15 nm Nd: YAG emission line is not resonant with an electronic absorption line of the main center *N* of Sm^{3+}, a perturbed spectral satellite, together with the concentration and electron-phonon broadening of the Sm^{3+} absorption lines could grant enough absorption to use these materials as ASE suppressors in the Nd: YAG lasers.

Acknowbdgements. This paper was supported by the Contract PN 09.39.02.01, 2011.

REFERENCES

1. J. B. Gruber, E. Hills, P. Nadler, ***M.*** R. Kokta, C A. Morrison, Chemical Physics, **113**, 175 (1987).
2. M. Malinowski, R. Wolski, Z. Frukacz, T. Lukasiewicz, Z. Luczynski, J. of Applied Spectroscopy, **62**, 839 (1995).
3. N. J. Hess, D. Shifer, J. Appl. Phys, **68**, 1953 (1990).
4. C. Sanchez-Valle, I. Daniel, B. Reynard, R. Abraham, C. Goutaudier, J. Appl. Phys., **92**, 4349 (2002).
5. V. Lupei, A. Lupei, A. Ikesue, Opt. Mat., **30**, 1781 (2008).
6. H. Yagi J.F. Bisson, K. Ueda, T. Yanagitani, Journal of Luminescence, **121,** 88(2006).
7. R.Huß, R. Wilhelm, C. Kolleck, J. Neumann, D. Kracht, Optics Express**, 18**, 13094 (2010).
8. T. Denis, S. Han, S. Mebben, R. Wilhelm, C. Kolleck, J. Neumann, D. Kracht, Applied Optics, **49**, 811 (2010)
9. R. M. Yamamoto, B. S. Bhachu, K. P. Cutter, S. N. Fochs, S. A. Lotts, C. W. Parks, T. F. Soules, Techn. Dig. OSA Adv. Solid-State Photonics, Nara 2008, paper WC5,
10. A. Ikesue, T. Kinoshita, K. Kamata, K. Yoshida, J. Am. Ceram. Soc., **78**, 1033 (1995).
11. A. Ellens, Phys. Rev. B, **55**, 180 (1997).
12. A. Lupei, Optical Materials, **16**, 153 (2001).
13. Y.K. Voronko, A.A. Sobol, Phys. Stat. Sol. A, **27**, 657 (1975).
14. V. Lupei, A. Lupei, C. Tiseanu, S. Georgescu, C. Stoicescu, P. M. Nanau, Phys. Rev. B. Condens. Mat., **95**, 8 (1995).
15. A. Lupei, V. Lupei and E. Osiac, J.Phys.:Cond. Matter, **10**, 9701 (1998).
16. A. Lupei, V. Lupei, Optical Materials**, 24**, 181 (2003).
17. V. Lupei, A. Lupei, S. Georgescu, T. Taira, Y. Sato, A. Ikesue, Phys. Rev. B, **64**, 092102 (2001).
18. V. Lupei, A. Lupei, A. Ikesue, J. Alloys. Comp., **380**, 61 (2004).